# Reconfigurable Antennas and Distributed Bit Loading for MIMO Ad-Hoc Networks

John Kountouriotis *Student Member, IEEE,* and Kapil R. Dandekar *Senior Member, IEEE*
Department of Electrical and
Computer Engineering
Drexel University
Philadelphia, PA 19104
Email: {jk368,dandekar}@drexel.edu

***Abstract*—In this work we evaluate the performance impact of reconfigurable antennas in a Multiple-Input Multiple-Output ad-hoc network where the links are allowed to transmit at the same time and interfere with each other. To achieve this goal, we have used two Reconfigurable Circular Patch Antennas (RCPA) to take channel measurements in a 3-link topology. To quantify the performance, instead of using Shannon capacity, we restrict the links to use an integer number of bits per transmission, with constraints on an application-imposed BER, as well as total available power per link. As the focus of this paper is on ad-hoc networks, we present iterative algorithms that achieve antenna configuration selection as well as bit and power loading in a distributed manner. By using an integer number of bits as well as SINR-based BER constraints, we aim to provide a realistic evaluation of the performance impact of reconfigurable antennas in a MIMO ad-hoc network.**

## I. Introduction

Reconfigurable antennas that are capable of dynamically changing their radiation pattern, have recently drawn a lot of attention for potential use in MIMO communication systems. Several reconfigurable antennas architectures have been proposed in the literature [1]–[6] and their performance in single link cases have been evaluated. The results show that reconfigurable antennas have the potential to increase achievable data rates in MIMO communication systems.

In this paper, we seek to quantify the practical performance impact of reconfigurable antennas in a MIMO ad-hoc network. Given that there is little to no published work that addresses this issue, we build upon [7]. In particular, we consider the performance in a MIMO ad-hoc network whose nodes are equipped with reconfigurable antennas and are restricted to use integer number of bits per transmission, so as to use symbols drawn from "practical" modulation constellations.

In order to address the practical considerations that the constraint of using only integer number of bits imposes, we borrow the framework and key ideas of bit loading that exist in the DSL literature [8]–[12]. Apart from this restriction in the integer number of bits, our work also differs from [7], in that there are channel measurements made to evaluate these techniques as opposed to ray-tracing simulations. For these channel measurements, actual reconfigurable antennas were constructed and evaluated.

The paper is organized as follows: In section II we present the reconfigurable antenna structure used for channel measurements. In section III we present the system model that we assume in this work, while in section IV we discuss the algorithm that we use to achieve a distributed bit loading and antenna configuration selection algorithm. Section V contains the measurement procedure we followed to obtain the data and evaluate system performance, while in section VI we present the results. Finally, in section VII the conclusions appear.

## II. Reconfigurable Circular Patch Antenna

The reconfigurable antenna array structure the authors consider in this work is the Reconfigurable Circular Patch Antenna (RCPA), which was first presented in [3]. It is a single element, two port circular antenna, that uses PIN diodes in order to dynamically change its radius. When the diodes are "off" electromagnetic mode $TM_{31}$ is excited ("Mode 3" configuration). When the diodes are "on", electromagnetic mode $TM_{41}$ is excited ("Mode 4" configuration). For completeness, the antenna schematic from [3] appears in Figure 1. By suitably placing the two feed ports in the structure, spatial orthogonality is achieved between the radiation patterns generated from each port, while maintaining a port isolation higher than $20\,dB$. The merits of this two-port single antenna, as well as the compact design relative to linear arrays, makes the RCPA suitable space-limited MIMO systems.

For the purposes of this work, two RCPA elements were built in order to be used at both the receiver and the transmitter during the channel measurements. Their radiation patterns in the azimuthal plane were measured in an anechoic chamber and appear in Figure 2. The calculations for the spatial correlation coefficients between the radiation patterns generated at the two ports, as well as between the patterns generated at the same ports for the different configurations for these build elements was very close to the simulated ones reported in [3] ($\leq 0.2$ for all cases) and the same holds for the radiation efficiency values ($\approx 20\%$ for Mode 3 and $\approx 6\%$ for Mode 4).

## III. System Model and Notation

Assume a $\mathcal{L}$ link network, with $\mathcal{L} = [1 \dots L]$. Further, we assume that all links are point-to-point MIMO links, with the intendend transmitter-receiver pairs pre-determined. We also assume that these links are co-located and interfere with each

978-1-4244-8180-4/10/$26.00 ©2010 IEEE

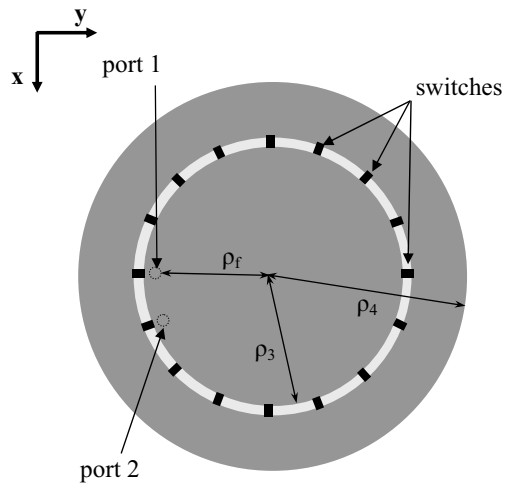


Fig. 1. Schematic of the Reconfigurable Circular Patch Antenna (RCPA)

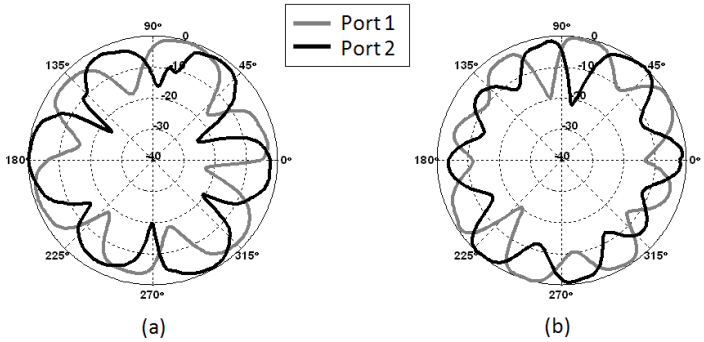


Fig. 2. Measured Pattern (in $dB$) in the azimuthal plane at the two ports of the RCPA in all its configurations for an operation frequency of $2.48\,GHz$:(a) port 1,"Mode 3", port 2 "Mode 3"; (b) port 1,"Mode 4", port 2 "Mode 4".

other. Each receiver and transmitter of link $i$ is equipped with a reconfigurable antenna array and we denote the configuration used by the receiver of link $i$ as $i_{rc}$ and the configuration used by the transmitter of link $i$ as $i_{tc}$. The channel matrix the receiver of link $i$ and the transmitter of link $j$ is denoted as $\mathbf{H}_{i_{rc},j_{tc}}$ and is naturally a function of the receive configuration of link $i$ and the transmit configuration of link $j$. Using $\mathbf{x}_i$ to denote the transmit symbol vector for link $i$ and under a flat fading assumption, we can write the signal received by the receiver of link $i$ as:

$$\mathbf{y}_i = \mathbf{H}\left(i_{rc}, i_{tc}\right)\mathbf{x}_i + \sum_{j\in\mathcal{L}\setminus i} \mathbf{H}\left(i_{rc}, j_{tc}\right)\mathbf{x}_j + \mathbf{n}_i \qquad (1)$$

where $\mathbf{n}_i$ is the noise vector at the receiver of link $i$ and we further assume that its elements are i.i.d circularly symmetric zero mean Gaussian random variables. Let $\mathbf{Q}_i$ denote the signal covariance matrix of link $i$ ($\mathbf{Q}_i = E\{\mathbf{x}_i\mathbf{x}_i^H\}$,"$\cdot^H$" the conjugate transpose). Then the power used by link $i$ is simply Trace$\{Q_i\}$. Without loss of generality, if we assume that the noise variance is unity, or equivalently if we express the transmit power normalized w.r.t. the noise power, we can write the interference plus noise covariance matrix that the receiver of link $i$ undergoes as:

$$\mathbf{R}_i = \mathbf{I} + \sum_{j\in\mathcal{L}\setminus i} \mathbf{H}\left(i_{rc}, j_{tc}\right)\mathbf{Q}_j\mathbf{H}\left(i_{rc}, j_{tc}\right)^H \qquad (2)$$

Notice that the interference plus noise covariance matrix of link $i$ is a function of the receive configuration of link $i$, as well as a function of all the transmit configurations used by the other links ($j_{tc}, j \in \mathcal{L}\setminus i$).

When the receiver of link $i$ can estimate $\mathbf{R}_i$ and the channel that carries the intended information (i.e. $\mathbf{H}\left(i_{rc}, i_{tc}\right)$) and a feed-back channel between the receiver and the transmitter exists, then the transmitter can use the singular value decomposition of *whitened channel* of link $i$ so as to precode its transmission. The whitened channel is defined as $\mathbf{Hw}_i\left(i_{rc}, i_{tc}\right) = \mathbf{R}_i^{-1/2}\mathbf{H}\left(i_{rc}, i_{tc}\right) = \mathbf{USV}^H$, with $\mathbf{USV}^H$ the singular value decomposition of $\mathbf{Hw}_i$ and $\mathbf{S}$ the real diagonal matrix with the singular values of $\mathbf{Hw}_i$ in its diagonal. Using $\mathbf{V}$, the transmitter can transmit the independent symbol vector $\mathbf{k}$ as $\mathbf{x}_i = \mathbf{Vk}$.

With this arrangement and after left-multiplication with $\mathbf{U}^H\mathbf{R}^{-1/2}$, the received signal in equation 1 becomes:

$$\tilde{\mathbf{y}}_i = \begin{bmatrix} s_1k_1 + \tilde{n_1} \\ \cdots \\ s_lk_l + \tilde{n_l} \\ 0 \\ \cdots \end{bmatrix} \qquad (3)$$

with $l$ being the number of non-zero elements (assuming descending order) of $\mathbf{S}$. Thus, $l$ ($l \leq \min\{N_t, N_r\}$, with $N_t$ and $N_r$ the number of transmit and receive elements) independent symbol streams are received, with the $i^{th}$ stream having an effective SINR of $|s_ik_i|^2$. The optimal power allocation in the above described scenario, is the waterfilling power allocation in [13], [14].

Obviously, when all the links in the network follow the same precoding and decoding operations [14], this procedure is an iterative one, with changes in the $\mathbf{x}$ vector in any of the nodes resulting in changes in the whitened channel of all other links. This technique is refered to as Multi-User Waterfilling or Iterative Waterfilling.

## IV. Distributed bit loading and antenna configuration selection

In our previous work [7], we have extended the basic Multi-User Waterfilling algorithm in [14] to accommodate the antenna configuration selection in the iterations as well. Here, we keep the main algorithm that was explained in [7], but instead of waterfilling over the singular values of the whitened channel, we perform bit-loading. The basic assumptions for the scheme to work are repeated here: At the beginning of each iteration the receiver of link $i$: *i.)*perfectly estimates the channel from the transmitter of link $i$ for all receive and transmit configurations, *ii.)* perfectly estimates $\mathbf{R}_i$ from equation 2 for all available receive configurations, *iii.)* can feed-back these observations to the transmitter of link

$i$ without any delay or errors. Furthermore, we assume the channels in the network do not change before convergence is achieved.

With each link having available transmit power $P_t$ at the beginning of iterations, the algorithm works as follows:

1) Initially a predetermined configuration is used for all the nodes in the network and for the first iteration all transmitters equally split all their available transmit power over their transmit elements. Each receiver in the network obtains the channel from its transmitter for all transmit and receive configurations, as well as $\mathbf{R}$ for all receive configurations.
2) Each link picks the receive configuration to be used, as well as the configuration for the transmitter, so as the resulting combination of $\mathbf{H}_i\left(i_{rc}, i_{tc}\right)$ and $\mathbf{R}_i$ would be the most capacity achieving, with the link taking into account the interference.
3) Performs bit loading over the non-zero singular values of the whitened channel matrix w.r.t BER constraints. Possible excess power, not enough to load one more bit, is not used. If the power available is not enough to load at least one bit, then the link refrains from transmissions.
4) While $\mathbf{Q}_i, i \in \mathcal{L}$ is changing, continue iteration until convergence.

For the bit-loading algorithm in step 3, we follow the approach from [8], [12]. Specifically, we construct a table with the values of power that need to be assigned to each stream in order to carry an additional bit, given some BER constraint. The required power is arranged in an increasing order and a bit is assigned to the singular value that requires the least amount of energy to carry this bit. The amount of power required to carry this bit is also assigned to the corresponding singular value and is subtracted from the total available power. The power required for the loaded singular value to carry one extra bit is calculated and the table is rearranged in increasing order. The iterations continue until there is no more power left to add an additional bit to any singular value, or until all singular values have the maximum number of bits loaded to them.

Notice here that the "channel gain" in our case, as is shown in equation 3, is $s_i^2$, with $s_i$ the $i^{th}$ diagonal element of $\mathbf{S}$. In other words the bit loading happens over spatial streams instead of frequency subchannels as in [8]–[12]. For the BER constraint, we make the assumption that the interference plus noise is gaussian and use standard BER constraints that appear in the literature [15].

### *A. Receiver Side Configuration Selection and Centralized Antenna Configuration Selection*

As in [7], apart from the case where the links are allowed to change configurations at both link ends, we also considered the case where only the receive antenna configurations are allowed to change. The reasoning for considering this scheme is the lower training required per iteration (less channels to estimate between the transmitter and the independent receiver) and the fact that configuration feedback to the transmitter is no longer required. But more important is the fact that the changes in the transmit configurations might result in higher interference imposed to other links, since the configuration selection is performed with respect to each individual links interest and not with respect to the overall impact in the network that this choice will have.

Apart from the two presented cases where the antenna configuration selection is performed in a distributed way (either on both link ends or at the receiver side only), we also consider centralized configuration selection in order to better quantify the upper-bound impact of reconfigurable antennas in a MIMO ad-hoc network.

For these centralized schemes, we assume that a powerful centralized controller exists that has knowledge of all channels for all configuration combinations and power allocations in the network. The central controller chooses the configuration combination to be used that would result in the maximum number of bits being transmitted from all links. In other words, the central controller runs the distributed bit loading algorithm for all possible configuration combinations, without allowing configuration switching during the iterations. After evaluating the outcome, in terms of number of bits being transmitted for all possible configuration combinations, it picks the configuration combination that resulted in the transmission of the most bits.

Apart from the scheme where the central controller evaluates all configuration combinations, we have also considered the scheme were the central controller evaluates the configuration combinations of the receivers only, while not changing the transmitter configurations so as to have an upper-bound for the corresponding distributed scheme as well.

## V. Measurement Set-up

As mentioned in section II, two RCPA elements were built and equipped with PIN diodes so as to use one two-port antenna element at the receiver and one at the transmitter for the channel measurements. The measured topology appears in Figure 3 and is in essence the same as the first of the three topologies that was simulated with a ray-tracing simulator in [7].

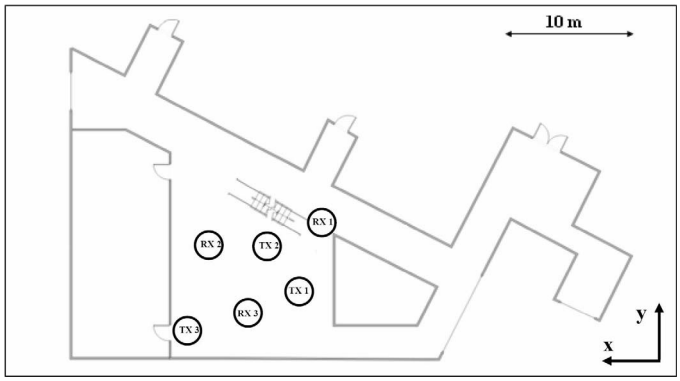


Fig. 3. Measured Topology

For the measurements we used the HYDRA Software Defined Radio platform, developed in collaboration with the

Wireless Networking & Communications Group at the University of Texas at Austin [16]. This platform was also used for the evaluation of reconfigurable antennas in single link scenarios [3], [17]. The platform is a $2\times2$ MIMO platform that operates in the 2.4 GHz band using OFDM with 64 subcarriers (52 are carrying data).

Three nodes (RX1 to RX3) with two receive elements each acted as receivers and three nodes (TX1 to TX3) with two transmit elements each acted as transmitters, so as to create 6 different network topologies, by pertubating the intended receiver-transmitter pairs. To capture small scale fading effects, the receive elements were placed on a robotic antenna positioner and were moved at 40 different positions at displacements of $\lambda/10$ along the y-axis for RX1 and RX2 and along the x-axis for RX3. At each position, 100 noisy channel estimates were captured and averaged for each subcarrier, so as to get the channel response between each receiver-transmitter pair at each point and subcarrier. The response at each subcarrier was treated as an independent narrow band channel realization. In this way, we acquired 12,480 samples (6 network topologies with 40 samples each and 52 subcarrier) of "network instances" to use for evaluation of the performance.

The acquired channels were normalized on a per subcarrier basis, so that for each subcarrier the stronger channel in the network (regardless of whether it is an intended or interfering channel) would have an expected (along the 40 points) squared frobenious norm equal to 4 (i.e. no path loss). All the channels for all configurations in each subcarrier were normalized with the same parameter, so as to attain relative strengths of channels and configurations. In other words, the normalization was performed so as $\forall s \in [1,\ldots,52]$, $\max_{l,i\in\mathcal{L},rc,tc} E\left\{|\mathbf{H}^s_{l_{rc},i_{tc}}||^2_F\right\} = 4$, with $s$ being the subcarrier index and the expectation taken over the 40 positions.

## VI. Results

Using the above described measured channels, we evaluated the distributed configuration selection and bit loading for the cases of switching both receive and transmit configurations ("Distributed") as well as when only the receive configuration is allowed to switch ("Distributed RX"). We also evaluated their corresponding centralized configuration selection schemes ("Centralized" and "Centralized RX"), as discussed in section IV-A. Apart from these schemes, we evaluated the case in which there is no configuration switching allowed and we call this case "Non-Reconfigurable". For the cases of Non-Reconfigurable, Distributed RX and Centralized RX, the link end(s) that are not allowed to switch configuration are restricted in using the most efficient configuration available (Mode 3).

The links were restricted to use symbols drawn from the constellations of BPSK and 4 to 64 QAM (i.e. they were allowed to have from 0 up to 6 bits with steps of one per symbol loaded in each singular value of the whitened channel). The uncoded BER constraint was set at $10^{-2}$. The total available power per link, normalized with respect to noise power (i.e. $P_t/\sigma^2$), ranged from 5 to 35 dB in steps of 5 dB.

### A. Throughput

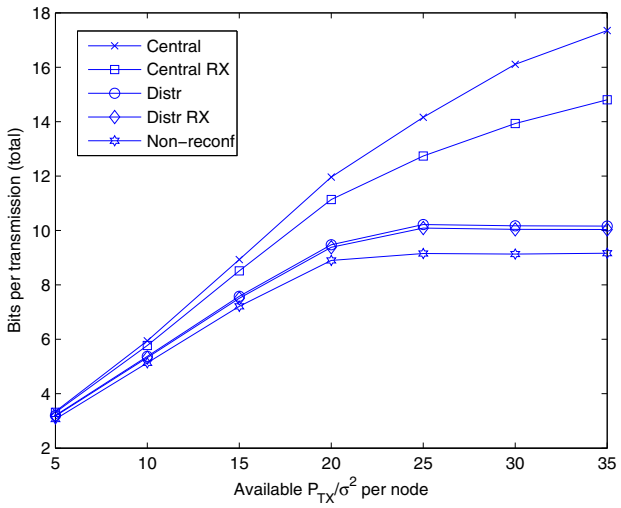


Fig. 4. Sum number of bits per transmission versus normalized available transmit power ($P_t/\sigma^2$)

In Figure 4 we see the average (over all network instances) number of transmitted bits for the schemes under consideration. In this figure we can see that compared to the Non-reconfigurable case there is some performance increase to be expected even when the configuration selection is performed in a distributed fashion. The increase in bits transmitted for $P_t/\sigma^2 = 25\,dB$ is $\approx 11.7\%$ between the Non-Reconfigurable and the Distributed cases. On the other hand, it seems that allowing configuration switching in a distributed fashion at both ends of the link does not yield much benefit, since the performance increase of the Distributed scheme versus the Distributed RX is only $\approx 1.3\%$ at $25\,dB$ $P_t/\sigma^2$.

But the true potential of the use of reconfigurable antennas is evident form the traces of the two centralized configuration selection schemes. The performance increase over the Non-reconfigurable case is $\approx 54.7\%$ for the Distributed scheme, while the Distributed RX achieves an increase of $\approx 39.1$ for $P_t/\sigma^2 = 25\,dB$. At the same available power levels, the centralized configuration selection schemes outperform their corresponding distributed ones by $\approx 26.2\%$ (RX case ) and by $\approx 38.5\%$. It is also of interest to notice that while the curve of the Non-Reconfigurable case "plateaus" at around $P_t/\sigma^2 = 20\,dB$ and the Distributed cases for around $P_t/\sigma^2 = 25\,dB$, the two centralized schemes seem to keep increasing even for $P_t/\sigma^2 > 35\,dB$, which in essence show the potential of the extra degrees of freedom the reconfigurable antennas offer in a MIMO ad-hoc network. These extra degrees of freedom allow the links to use configurations that would not only provide a strong channel between the receiver and

the transmitter, but would also mitigate interference and thus would enhance the SINR seen by each link.

### B. Solution Stability

In this section we try to quantify how much the resulting bit allocation is sensitive to changing initial antenna configuration (the configurations that the iterations start with). For this task, we evaluated the algorithm outcome for the $40 \times 52$ network instances of topology 1 for all 64 possible initial configuration assignments and for all 7 available power levels, for the Distributed case.

In order to quantify the "spread" of the resulting bit allocations, we used the average absolute deviation from the mean metric, which is defined as

$$d = \frac{1}{n} \sum_{i=1}^{n} |b_i - \overline{b_i}| \tag{4}$$

with $n$ the number of samples available, $b_i$ the the values whose "spread" we wish to calculate and $\overline{b_i}$ their average value. We were interested to see how much the resulting solutions vary for each of the network instances when the initial configuration selection changes but also look into how much the average (over the network instances) solution would vary with changing initial configurations.

In Figure 5 we plot the expected average absolute deviation from the mean, with $b_i$ the sum bit allocation capacity of each instance (Instance Sum Bit Deviation), as well as the average absolute deviation of the average sum bit allocation, with $b_i$ the average sum bit allocation over these instances(Average Sum Bit Deviation) for each initial configuration combination.

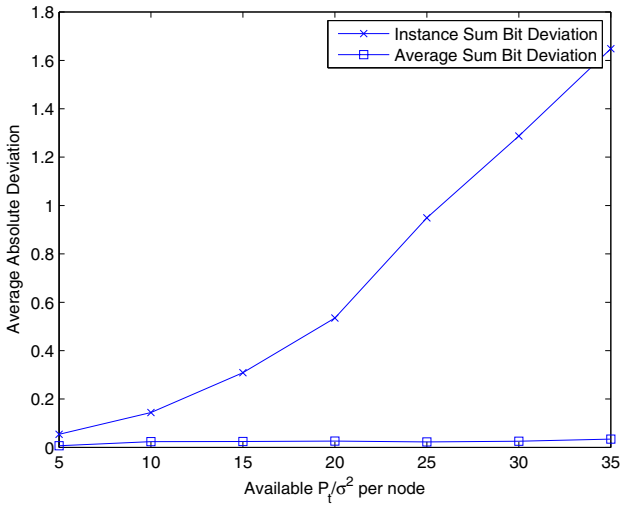


Fig. 5. Instance and Average sum bit absolute deviation of the Distributed solution with varying initial configurations

From the plot we see that while there are some differences to be expected of the resulting solutions on a per instance level (Instance Sum Bit Deviation trace), especially for increasing available power, the average sum bit solution (Average Sum Bit Deviation trace) remains practically the same ($d < 0.035$) when the configurations with which the iterations start change. These results imply that while the bit loading and configuration solutions are sensitive to initial conditions, overall throughput performance is not significantly impacted.

### C. Number of Links Transmitting and Percentage Power Used

Since we do not require the links to use their full power, but rather allow them to use exactly the amount of power needed to meet the BER constraint imposed, it is expected that some power will remain unused. In this section we answer the question of what fraction of available power is used on average for each technique discussed. Further, given that it is not necessary that all links will be able to transmit depending on their effective SINR, it is also of interest to look into how many users are transmitting per slot on average.

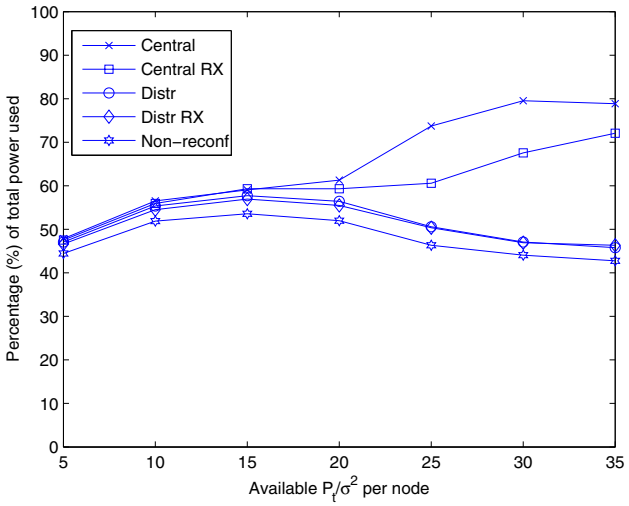


Fig. 6. Percentage of Available Power Used

In Figure 6 we plot the percentage of the total available power used by the links and in Figure 7 we plot the average number of transmitting links. For the two centralized configuration selection techniques, we see that the percentage of power used is always higher than the corresponding distributed techniques, which is also reflected in Figure 4. On the other hand, we see that for $P_t/\sigma^2 < 25\,dB$ the number of transmitting users is smaller for the centralized cases than for the distributed case. We also see that only for higher available transmit powers the number of transmitting users for the centralized techniques becomes greater than in the distributed scenarios.

For low available transmit powers, the centralized configuration selection often results in configurations in which 2 of the 3 links will be transmitting, using most of their available power ($\approx 75\%$ each). It is only for the higher available power that the configurations selected will allow all three links to transmit, again using most of the available power.

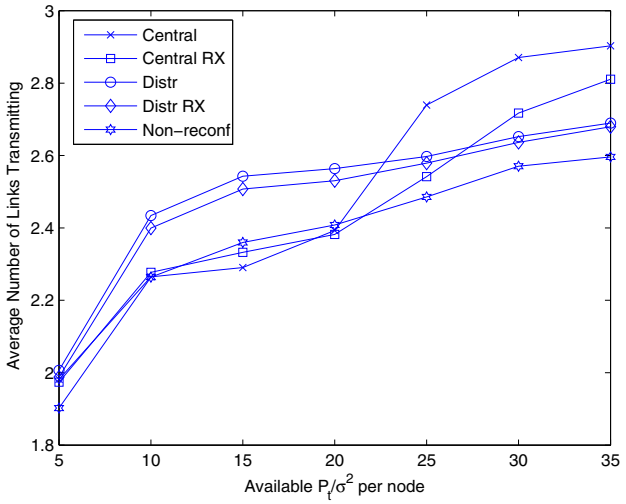


Fig. 7. Average Number of Links Transmitting

On the other hand, with the distributed configuration selection, each link will selfishly choose a configuration that would provide a higher chance of transmitting, regardless of the interference level that is imposed on the other links. This is why a greater number of links transmit, compared with the centralized case, in the lower range of available powers. At the higher range of available transmit powers, the number of transmitting links becomes smaller than in the centralized scheme due to the higher interference levels the selfish configuration selection leads to. Furthermore, the distributed configuration selection leads to under-utilization of the available power for the entire range of available powers considered, as compared to the centralized case. When compared to the Non-reconfigurable case though, the distributed configuration selection schemes uses more power and allows more links to transmit for all considered available power range.

## VII. Conclusion

In this work we aimed at evaluating the performance impact to be expected from using reconfigurable antennas in a MIMO ad-hoc network. We considered practical system constraints by allowing integer number of bits to be used forming symbols from practical modulation constellations while respecting BER and transmit power constraints. We presented a distributed algorithm for configuration selection and bit loading and compared its performance to the case where there is a centralized controller performing the configuration selection. Results showed that even with these practical considerations imposed to the system, there are considerable performance benefits to be expected by using reconfigurable antennas in a MIMO ad-hoc network, compared to the Non-reconfigurable case. The results of the centralized configuration selection schemes motivates the development of a more sophisticated selection algorithm to exploit the full potential of the reconfigurable antennas in a MIMO ad-hoc network.

## Acknowledgment

This material is based upon work supported by the U.S. National Science Foundation under grants 0916480 and 0322795.

## References

[1] D. Piazza, N.J. Kirsch, A. Forenza, Jr. Heath, R.W., and K.R. Dandekar, "Design and evaluation of a reconfigurable antenna array for MIMO systems," *IEEE Transactions on Antennas and Propagation*, vol. 56, no. 3, pp. 869 – 881, 2008.

[2] J. D. Boerman and J. T. Bernhard, "Performance study of pattern reconfigurable antennas in MIMO communication systems," *IEEE Transactions on Antennas and Propagation*, vol. 56, no. 1, pp. 231 – 236, 2008.

[3] D. Piazza, P. Mookiah, M. D'Amico, and K.R. Dandekar, "Two port reconfigurable circular patch for MIMO systems," *Proceedings of the 2007 European Conference on Antennas and Propagation (EuCAP)*, 2007.

[4] B.A. Cetiner, E. Akay, E. Sengul, and E. Ayanoglu, "A MIMO system with multifunctional reconfigurable antennas," *IEEE Antennas and Wireless Propagation Letters*, vol. 5, no. 31, pp. 463 – 466, 2006.

[5] A. Grau, H. Jafarkhani, and F. De Flaviis, "A reconfigurable multiple-input multiple-output communication system," *Wireless Communications, IEEE Transactions on*, vol. 7, no. 5, pp. 1719–1733, May 2008.

[6] A.M. Sayeed and V. Raghavan, "Maximizing MIMO capacity in sparse multipath with reconfigurable antenna arrays," *IEEE Journal of Selected Topics in Signal Processing*, vol. 1, no. 1, June 2007.

[7] J. Kountouriotis, D. Piazza, P. Mookiah, M. D'Amico, and K.R. Dandekar, "Reconfigurable antennas for mimo ad-hoc networks," in *Radio and Wireless Symposium, 2008 IEEE*, 22-24 2008, pp. 563 –566.

[8] Jorge Campello De Souza, *Discrete bit loading for multicarrier modulation systems*, Ph.D. thesis, Stanford University, Stanford, CA, USA, 1999, Adviser-Gill,III, John T.

[9] P. S. Chow, J. M. Cioffi, and J. A.C. Bingham, "Practical discrete multitone transceiver loading algorithm for data transmission over spectrally shaped channels," *IEEE Transactions on Communications*, vol. 43, no. 2-4, pp. 773 – 775, 1995.

[10] Lee. J., R.V. Sonalkar, and J.M. Cioffi, "Multiuser bit loading for multicarrier systems," *Communications, IEEE Transactions on*, vol. 54, no. 7, pp. 1170 –1174, july 2006.

[11] S. Jagannathan and J.M. Cioffi, "Distributed adaptive bit-loading for spectrum optimization in multi-user multicarrier systems," in *Communications, 2008. ICC '08. IEEE International Conference on*, 19-23 2008, pp. 625 –630.

[12] J.A.C. Bingham, "Multicarrier modulation for data transmission: an idea whose time has come," *IEEE Communications Magazine*, vol. 28, no. 5, pp. 5 – 14, 1990.

[13] R. S. Blum, "MIMO capacity with interference," *IEEE Journal on Selected Areas in Communications*, vol. 21, no. 5, pp. 793 – 801, 2003.

[14] M.F. Demirkol and M.A. Ingram, "Power-controlled capacity for interfering MIMO links," *IEEE Vehicular Technology Conference*, vol. 1, no. 54D, pp. 187 – 191, 2001.

[15] B. P. Lathi, *Modern Digital and Analog Communication Systems, 3rd Edition*, Oxford University Press, 1998.

[16] A. Gupta, A. Forenza, and R. W. Heath Jr., "Rapid MIMO-OFDM software defined radio system prototyping," in *IEEE Workshop on Signal Processing Systems, SiPS: Design and Implementation*, Austin, TX, United States, 2004, pp. 182 – 187.

[17] D. Piazza and K.R. Dandekar, "Reconfigurable antenna solution for MIMO-OFDM systems," *Electronics Letters*, vol. 42, no. 8, pp. 15 – 16, 2006.